

# Blade-Vortex Interaction

David R. Poling\* and Leo Dadone†

*Boeing Helicopter Company, Philadelphia, Pennsylvania*  
and

Demetri P. Telionis‡

*Virginia Polytechnic Institute and State University, Blacksburg, Virginia*

**A conformal transformation and discrete vortex dynamics are used to calculate the interaction of a blade with vortices drifting with the freestream. An unsteady Kutta condition is employed to estimate the strength of vortices shed at the trailing edge. Instantaneous pressure distributions are calculated and compared with earlier experimental and analytical data.**

## Introduction

THE vorticity trailed by finite wings and rotor blades rolls up and develops into almost ideal vortex filaments. When wings, control surfaces, or helicopter blades encounter such vortices, the ensuing interaction influences greatly the aerodynamic performance and vibratory airloads experienced by the aircraft. Moreover, it was found that aerodynamic interaction of a vortex and a blade may generate impulsive noise as at high speed, in descent, and during some maneuvers. Complex rotor codes have been developed that use lifting-line theory to calculate blade airloads and rotor performance. The results for a typical, instantaneous wake model are shown in Fig. 1 to illustrate the relative positions of the trailed vorticity on the computation blade. The two-dimensional counterpart of this, i.e., the parallel vortex interaction with the blade, has recently been examined both theoretically and experimentally.

In two-dimensional modeling usually it is assumed that the vortex is parallel to the airfoil axis and drifts from far upstream. Inviscid theories as well as full Navier-Stokes equations have been employed. Significant advances have been made in transonic flow problems.<sup>1-5</sup> The incompressible flow problem has also been studied,<sup>6,7</sup> and later, Hsu and Wu<sup>8</sup> presented both discrete-vortex solutions as well as full Navier-Stokes solutions to the problem. Most recently, Mook and Alexander<sup>9</sup> refined their method of vortex splitting to calculate the interaction of two airfoils in close proximity. Panaras<sup>10</sup> also investigated the problem of blade-vortex interaction by modeling the oncoming vortices in terms of clouds of point vortices.

On the experimental side, a number of contributions have been centered around the noise generated during the interaction process. Two recent investigations that also refer to earlier work<sup>11,12</sup> reported on the lift history as well as instantaneous pressure distributions, but only for the 20% forward portion of the chord. Favier et al.<sup>13</sup> reported complete sets of instantaneous profiles, but their oncoming vortices were generated by a periodically stalling airfoil that would not be easy to model analytically. Poling and Telionis<sup>14</sup> also report results on the interaction of vortices with an airfoil but limit their data to the trailing-edge region. Rockwell and his associates, on the other hand, have been examining the interaction of vortices with sharp leading edges (see, e.g., Ref. 15).

In the present paper we discuss an incompressible, inviscid numerical method capable of calculating the interaction of a two-dimensional airfoil with discrete and periodically spaced oncoming vortices. Whereas Basu and Hancock<sup>16</sup> and Kim and Mook<sup>17</sup> employed a panel approximation in the calculation of the flow about pitching airfoils, the present work employs a conformal transformation method. The interaction of a NACA 0012 airfoil with a single oncoming vortex as well as a sequence of vortices is investigated. The results are compared with earlier experimental and analytical data.

## Theoretical Considerations

The first attempt to estimate unsteady forces due to viscous wakes was presented by Kemp and Sears.<sup>18</sup> In fact, Sears, to whom the present article is dedicated, essentially opened the area of unsteady airfoil aerodynamics in the late 1930's.<sup>19,20</sup>

The present analytical scheme is based on discrete vortex dynamics and on the circle theorem as outlined in Milne and Thomson.<sup>21</sup> By virtue of Joukowski's transformation

$$\zeta(z) = z + (a^2/z) \quad (1)$$

the unsteady flowfield over a circular cylinder in the  $z$  plane is mapped into a Joukowski airfoil in the  $\zeta$  plane or physical plane. In response to changing events, a vortex is shed and the bound vorticity is readjusted. The shed vortex is placed at an arbitrary distance slightly downstream of the trailing edge.

Depending on the position and radius of the circle in the  $z$  plane, a variety of shapes in the  $\zeta$  plane may be obtained. In the initial stages of the work it was decided to use a NACA 0012 airfoil in the computation scheme, since results from a finite trailing-edge wedge angle would correlate better with test data than would a trailing edge with a cusp. Therefore, it was necessary to adjust the radius of the image circle and its position in the  $z$  plane until the shape in the  $\zeta$  plane represented very nearly that of a NACA 0012 airfoil. The Joukowski airfoil thus employed has a trailing-edge radius of curvature equal to that of a NACA 0012, namely, 0.5% of the chord length, and coordinates no different than 1% of chord when compared with a NACA 0012. The corresponding quantities of the circular cylinder in the  $z$  plane, namely, the radius of the circle and the Cartesian coordinates of its origin, are 1.111, 0.079, and 0.00, respectively.

In order to render the solution unique at each time step, a generalized Kutta-Joukowski condition at the trailing edge was imposed. The condition employed here was essentially the one proposed by Giesing.<sup>22</sup> This is similar to the condition employed by Ham,<sup>23</sup> Mathioulakis and Telionis,<sup>24</sup> and Kim and Mook.<sup>17</sup> Experimental confirmation of this condition and further discussion of the topic can be found in Refs. 25 and 26. In a more recent publication, Hsu and Wu<sup>7</sup> propose an alternative condition that in principle determines both the inclination and

Received March 23, 1987. Copyright © American Institute of Aeronautics and Astronautics, Inc., 1988. All rights reserved. This paper is dedicated to Professor W. R. Sears on the occasion of his 75th birthday.

\*Technical Specialist, Aeromechanics. Member AIAA.

†Supervisor, Aeromechanics. Member AIAA.

‡Professor. Associate Fellow AIAA.

the magnitude of the velocity downstream of a trailing edge.

The flow over an airfoil of a stream containing one or more drifting vortices can be calculated in the image plane by superimposing the elementary solutions of a uniform stream, a doublet, and vortices. In dimensionless quantities, the complex potential in the  $z$  plane becomes

$$F(z) = -ze^{i\alpha} - \frac{e^{-i\alpha}}{z} + i\Gamma\ell n z + i \sum_{q=1}^N \Gamma_q [\ell n(z - z_q) - \ell n(\bar{z} - \bar{z}_q)] \quad (2)$$

where  $\Gamma$  and  $\Gamma_q$  represent the circulation around bound and free vortices, respectively, and  $\alpha$  is the angle of attack in the physical plane. In this equation, lengths and circulations are rendered dimensionless in terms of the radius of the cylinder  $R$  and the quantity  $2\pi RU_\infty$ , respectively, with  $U_\infty$  the freestream velocity. The terms with overbars in Eq. (2) denote complex conjugate quantities. The condition of no penetration on the surface of the cylinder is satisfied by placing two vortices inside the circle for each vortex in the flowfield. One vortex is placed at the center of the circular cylinder and another at the conjugate point, namely, the point at  $1/\bar{z}_q$ .

The  $z$ -plane complex velocity  $w(z)$  expressed in terms of the complex potential function reads

$$w(z) = \frac{d}{dz} F(z) = -e^{i\alpha} + \frac{e^{-i\alpha}}{z^2} + \frac{i}{z} + i \sum_{q=1}^N \Gamma_q \times \left( \frac{1}{z - z_q} - \frac{1}{z - (1/\bar{z}_q)} + \frac{1}{z} \right) \quad (3)$$

### Numerical Analysis

The initial flowfield is calculated via Eq. (2), where  $N$  takes the value 1 or 20 for the interaction of the blade with one or a street of 20 vortices, respectively. In the first case, the free vortex is positioned a few chord lengths upstream of the blade (see Fig. 2). In the second case, the blade is positioned in the middle of the street (see Fig. 3). The solution then proceeds in increments of time  $\Delta t$ . Vortices are allowed to drift with the flow. They are displaced by increments equal to the product of the local velocity times  $\Delta t$ . At each instant, the bound circulation is allowed to readjust, and a new vortex is released at the trailing edge to simulate the shedding of vorticity.

At each time step, the number of vortices simulating the wake increases by 1. The two unknowns, the instantaneous value of bound circulation  $\Gamma$  and the strength of the nascent vortex  $\Gamma_N$ , are determined by virtue of the unsteady Kutta condition and the conservation of the total amount of circulation:

$$-e^{i\alpha} + \frac{e^{-i\alpha}}{z_{te}^2} + \frac{i\Gamma}{z_{te}} + i \sum_{q=1}^N \Gamma_q \left( \frac{1}{z_{te} - z_q} - \frac{1}{z_{te} - (1/\bar{z}_q)} + \frac{1}{z_{te}} \right) = 0 \quad (4)$$

$$\Gamma + \sum_{q=1}^N \Gamma_q = 0 \quad (5)$$

The subscript  $te$  denotes the location on the circle that corresponds to the trailing edge of the airfoil.

The velocity of the  $q$ th vortex at any point in the  $z$  plane is obtained from the equation

$$w_q = w - (i\Gamma_q/z - z_q) \quad (6)$$

where  $w$  is given by Eq. (3). This is the condition for a free-force vortex. This type of vortex is convected with the local velocity. In the computer program, a cutoff statement was used when two or more vortices approached one another. If the

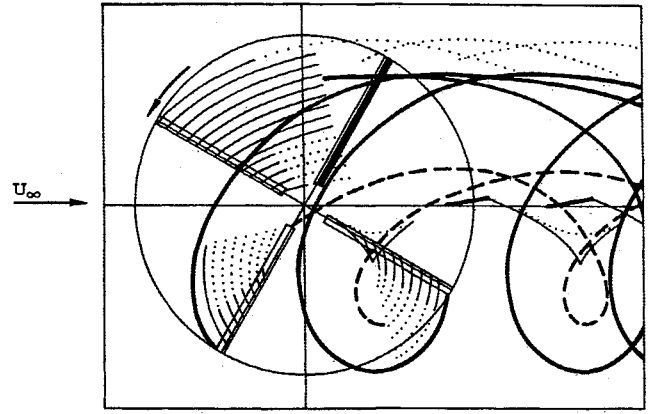


Fig. 1 Instantaneous rotor wake model obtained via lifting-line theory; thick solid lines represent outboard tip vortices, dashed lines represent inboard tip vortices, and dots represent trailing-edge vortex sheets.

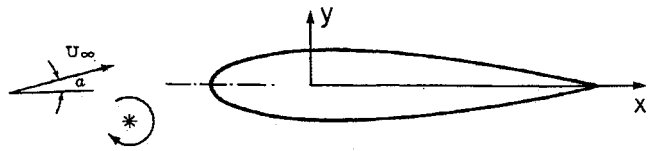


Fig. 2 Two-dimensional blade-vortex interaction; unsteady flow over an NACA 0012 airfoil at an angle of attack of 5 deg.

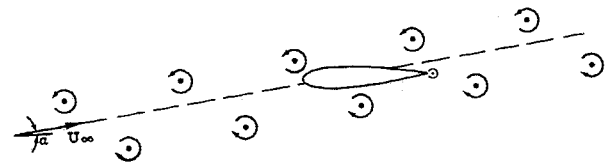


Fig. 3 Initial configuration of an undisturbed sequence of alternating vortices over an NACA 0012 by Joukowski transformation; the angle of attack is 5 deg.

positions of two vortices were within a small distance  $\epsilon$  of each other,

$$|z_q - z| \leq \epsilon \quad (7)$$

the computer program would skip that calculation and continue until the difference of any two neighboring positions was outside of this limit. The parameter  $\epsilon$  was chosen to be 0.05. This scheme was employed because artificially high velocities would occur in the neighborhood where vortices gather. Several other schemes have been developed in the past to avoid this particular problem. A description of different methods and their relative success can be found in Ref. 27. It should be emphasized that a variety of techniques discussed by these authors are designed to predict accurately the rolling up of free shear layers at large times. This is not the aim here. We are rather interested in the effect of free disturbing vortices on the instantaneous pressure distribution on the airfoil.

The convection of the vortices at each time step was performed via the equation

$$z_q(t + \Delta t) = z_q(t) + w_q(z_q, t) \cdot \Delta t \quad (8)$$

where  $\Delta t$  is the time increment and  $z_q(t + \Delta t)$  is the new position of the corresponding vortex. The value of the parameter  $\Delta t$  ranged from 0.05 to 0.30.

The initial positions of the vortices in the  $z$  plane  $z_q(t)$  correspond directly to positions in the  $\zeta$  plane  $\zeta_q(t)$  through the conformal transformation. However, positions at the second time step and time steps thereafter, namely,  $z_q(t + \Delta t)$  and  $\zeta_q(t + \Delta t)$ , are not image points of each other. Routh's theorem dictates that the path of a vortex in the  $z$  plane does not follow

the same path of the corresponding vortex in the  $\zeta$  plane. According to Routh's theorem, the vortices in the  $\zeta$  plane are convected by the equation

$$\zeta_q(t + \Delta t) = \zeta_q(t) + \frac{w_q(z_q, t)}{\frac{d\zeta}{dz}\big|_{z=z_q}} + i\Gamma_q \frac{d}{d\zeta} \ell n \frac{1}{\frac{d\zeta}{dz}\big|_{z=z_q}} \cdot \Delta t \quad (9)$$

The classical formula for lift,  $\rho U_\infty \Gamma$  is not valid in unsteady, attached, or separated flow. Thus, flows of this nature require direct integration of the pressure distribution. The Bernoulli equation in its nondimensional unsteady form reads

$$p = 1 - \frac{2}{R} \frac{\partial \Phi}{\partial t} - |w_s|^2 \quad (10)$$

where  $w_s$  is the velocity on the surface of the blade. This employs the potential function that is the real part of the complex potential  $F(z)$ . The partial derivative  $\partial \Phi / \partial t$  at a time  $t$  is approximated by the following equation:

$$\frac{\partial \Phi}{\partial t} \bigg|_t = \frac{\Phi|_t - \Phi|_{t-\Delta t}}{\Delta t} \quad (11)$$

The pressure distribution is determined using 180 points positioned around the surface of the airfoil. At each of these points, the pressure  $p$  is determined and then plotted with respect to the airfoil chord.

### Results and Discussion

All the results presented in this paper are displayed in terms of a Cartesian system of coordinates, aligned with the freestream, with its origin at the leading edge of the airfoil. Lengths are rendered dimensionless with the chordlength of the airfoil.

Typical instantaneous pressure distributions and corresponding vortex positions are shown in Figs. 4 and 5 for interaction with single and multiple vortices, respectively. In both cases, the airfoil is positioned at an angle of attack of  $\alpha = 5^\circ$ . Figure 4 displays the trajectory of the oncoming vortex and the configuration of the trailing vortex sheet for a vortex of strength  $\Gamma = -0.035$  released at the point  $x/c = 1$ ,  $y/c = -0.25$ . Figure 5 shows a similar behavior, 17 time steps after the airfoil was suddenly immersed in the middle of the vortex street and then allowed to interact with it. In both figures it appears that the airfoil tends to push away the oncoming vortex on both its sides. Moreover, a free vortex distorts the shape of the trailing-edge vortex sheet as shown in Fig. 5. Vortex imprints can be identified on the pressure side of the blade in both figures.

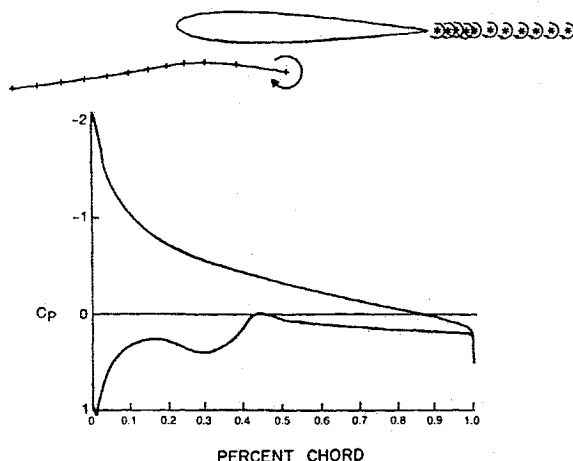


Fig. 4 Vortex trajectory and corresponding pressure distribution; the angle of attack is 5 deg, the nondimensional vortex strength  $\Gamma$  is  $-0.035$  clockwise, and the vortex release point is  $x/c = -1$ ,  $y/c = -0.25$ .

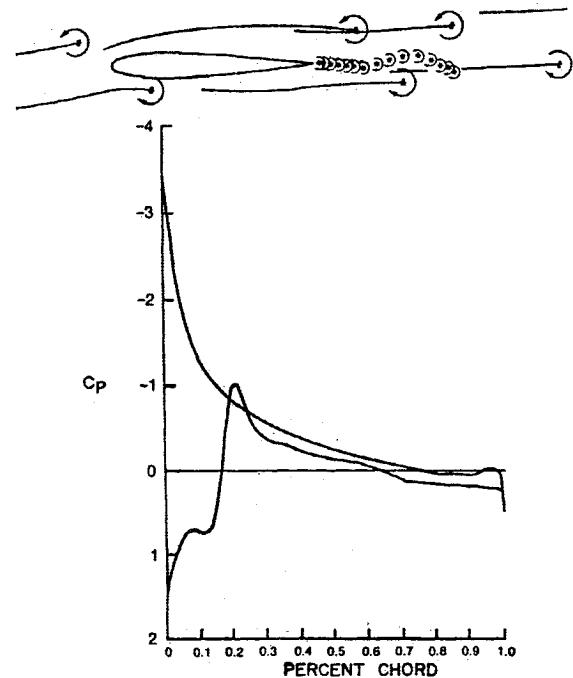


Fig. 5 Multiple vortex flow and corresponding pressure distribution; the angle of attack is 5 deg, and the nondimensional vortex strength  $\Gamma$  is 0.1.

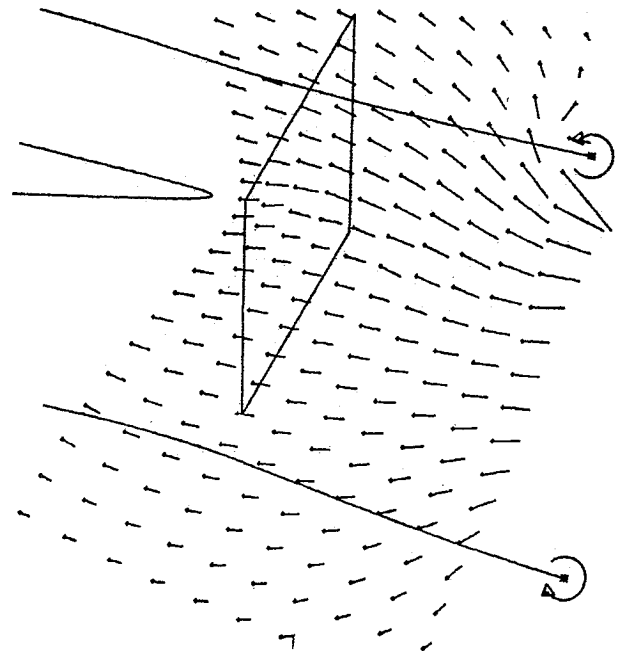


Fig. 6 Instantaneous velocity field in the vicinity of the trailing edge.

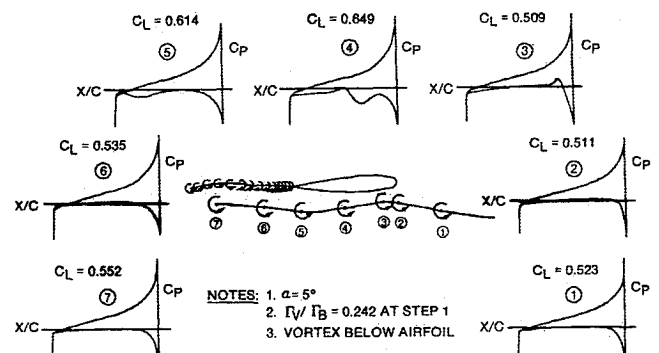


Fig. 7 Instantaneous pressure distributions from two-dimensional modeling of blade-vortex interaction; the angle of attack is 5 deg, and the vortex release point is  $x/c = -1$ ,  $y/c = -0.25$ .

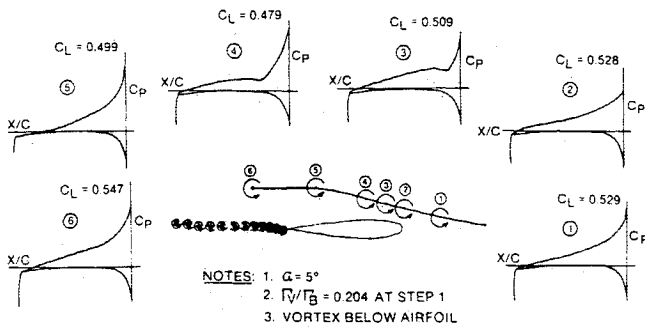


Fig. 8 Instantaneous pressure distribution from two-dimensional modeling of blade-vortex interaction; the angle of attack is 5 deg, and the vortex release point is  $x/c = -1$ ,  $y/c = 0$ .

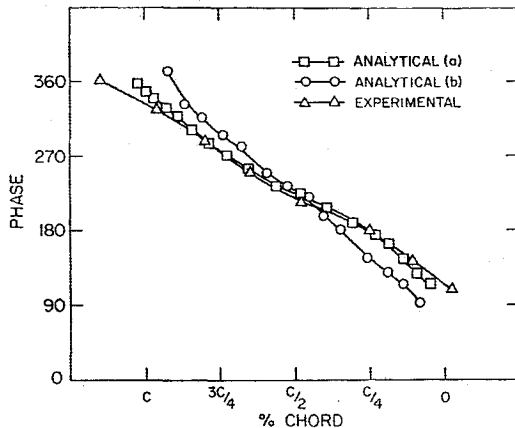


Fig. 9 Temporal trajectories of vortices over airfoil for a street of 20 vortices calculated with a) 20 free vortices and b) 4 free vortices.

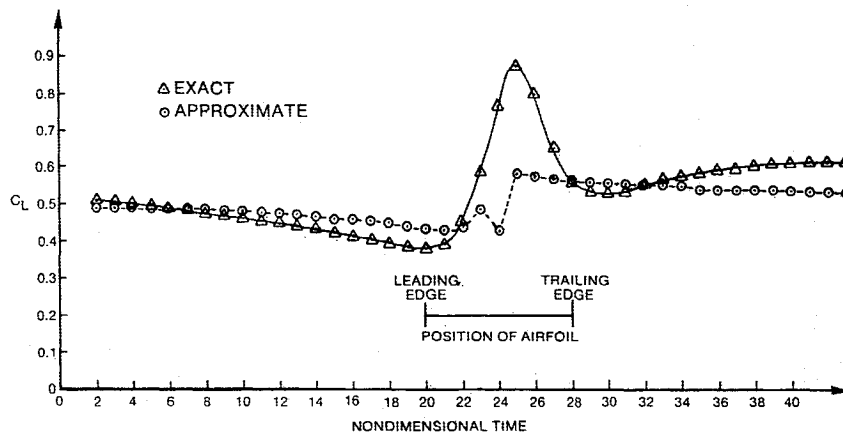


Fig. 10 Variation of lift coefficient from blade-vortex interaction; potential flow model of the passage of a vortex over a NACA 0012; path of vortex is below the blade; the vortex release point is  $x/c = -1.15$ ,  $y/c = -0.50$ .

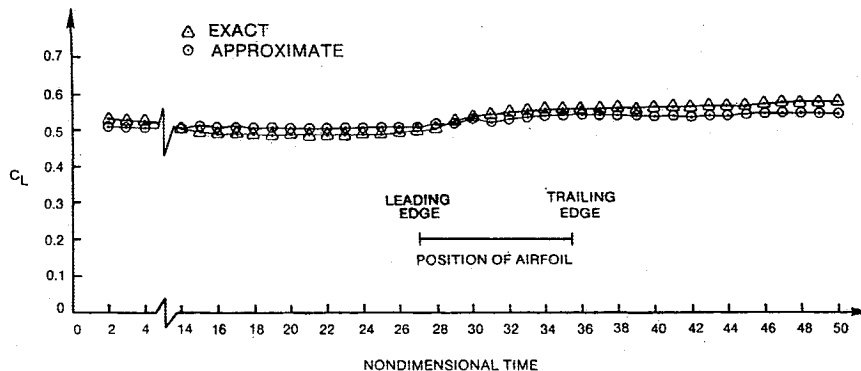


Fig. 11 Variation of lift coefficient from blade-vortex interaction; potential flow model of the passage of a vortex over a NACA 0012; path of vortex is below the blade; the vortex release point is  $x/c = -3$ ,  $y/c = -1.25$ .

A detail of the velocity field in the neighborhood of the trailing edge is displayed in Fig. 6. In this figure, the locations of the vortices are also depicted. Attention should be focused in the immediate vicinity of the edge where at this instant the velocity appears aligned with the bottom surface, in agreement with the unsteady Kutta condition.<sup>25</sup>

Sequences of instantaneous pressure distributions for interaction with a single oncoming vortex are displayed in Figs. 7 and 8 for a strength of a free-vortex-to-bound-vortex ratio of  $\Gamma_v/\Gamma_B = 0.204$ , where  $\Gamma_B$  is the undisturbed circulation of the airfoil at  $\alpha = 5$  deg. The vortex is released at  $x/c = 1$ ,  $y/c = -0.25$  and  $x/c = 1$ ,  $y/c = 0$  for the two cases, respectively. The vortex imprint can be identified on the pressure or suction side of the airfoil for Figs. 7 and 8, respectively, as the free vortex drifts from the leading to the trailing edge of the airfoil. The corresponding instantaneous values of the lift coefficient are also shown.

For the case of an airfoil immersed in a vortex street, the time record of vortex positions was calculated for a total of 4 or 20 disturbing vortices. The results are displayed in Fig. 9 together with the experimental data of Ref. 26.

Practically all comprehensive rotor codes employ lifting-line methods to evaluate local airloads along a rotor blade. A typical rotor performance and airload analysis is described in Ref. 28. For unsteady flows of the type shown here, lifting-line theory does not account for all changes taking place during the close encounter between the vortex and the airfoil. The lifting-line approach used in the rotor analysis of Ref. 28 calculates the lift variation by looking up two-dimensional tables of sectional characteristics. This is referred to as the "approximate" curve in Figs. 10 and 11. To compare the results of this theory with the present method, we calculated the history of the lift variation for a  $\alpha = 5$  deg. Lift was calculated by integrating the pressure distribution as described in the previous section. Figures 10 and 11 show the comparison for vortices released at

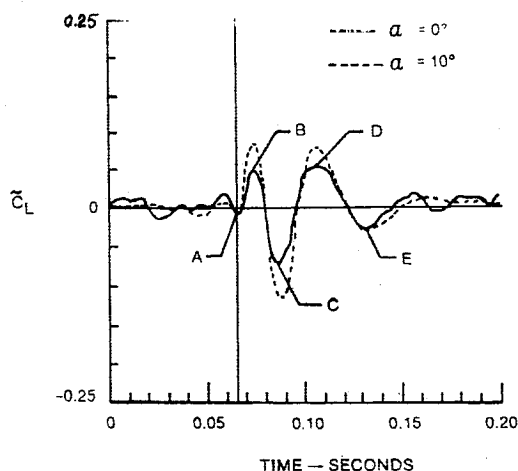


Fig. 12 Perturbation lift-time history of Ref. 12; nondimensional vortex strength and time in Figs. 13 and 14 correspond to the same conditions used in Ref. 12.

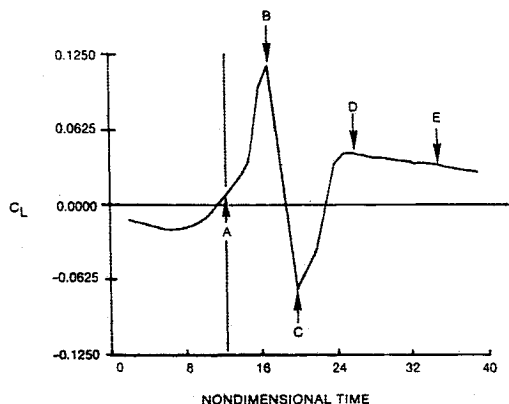


Fig. 13 Calculated lift-time history from the blade-vortex interaction as shown in Fig. 14; characteristic points are marked with the same notation as shown in Fig. 12.

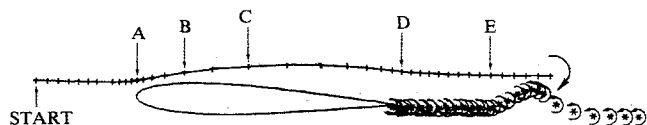


Fig. 14 Trajectory and vortex position over the upper surface of the NACA 0012; the angle of attack is 0 deg, the nondimensional vortex strength  $\Gamma_v$  is  $-0.05$  clockwise, and the vortex release point is  $x/c = -0.75$ ,  $y/c = 0.2$ .

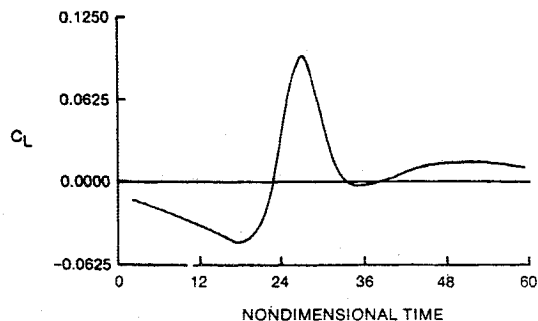


Fig. 15 Lift-time history corresponding to the same conditions as shown in Fig. 16, Ref. 8; the angle of attack is 0 deg, the nondimensional circulation strength  $\Gamma$  is  $-0.042$  clockwise, and the vortex release point is  $x/c = -1.25$ ,  $y/c = -0.25$ .

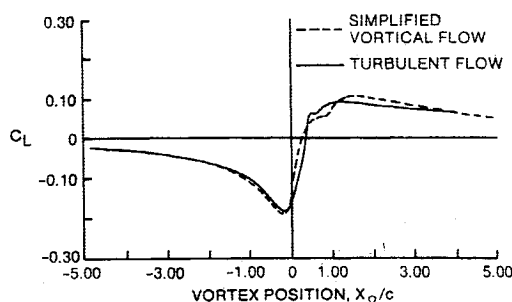


Fig. 16 Lift-time history as shown in Fig. 6 of Ref. 8.

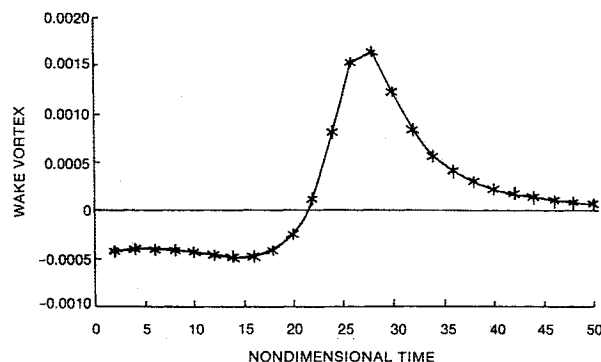


Fig. 17 Time history of nascent vortex strength corresponding to the same conditions as shown in Fig. 18 of Ref. 8.

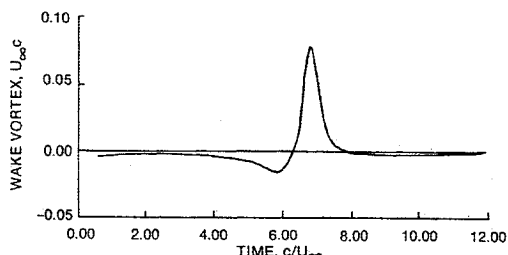


Fig. 18 Time history of vortex shedding as shown in Fig. 4 of Ref. 8.

$x/c = 2.25$ ,  $y/c = -0.50$  and  $x/c = 3$ ,  $y/c = -1.25$ , respectively. Lifting-line theory is quite adequate if the drifting vortex does not come within one chord length of the airfoil. However, it fails to predict the behavior of lift if the vortex passes a distance less than one chord length from the airfoil.

This type of temporal variation of the lift was compared with the experimental results of Booth<sup>12</sup> (see Fig. 12) for an angle of attack of  $\alpha = 0$  deg. Characteristic peaks are marked in Fig. 13 with the notation of Fig. 12 of Booth.<sup>12</sup> There appears to be good agreement on the values of times at which the event of lift peaking occurs. However, the magnitude of lift peaks are not estimated correctly. This may be due to various factors. Perhaps most important is the fact that in reality the vortex is actually cut by the blade. This is not modeled by the theory, which requires that the vortex be allowed to proceed on one of the two sides of the airfoil, as shown in Fig. 14. (Further developments in this direction appeared recently.<sup>29, 30</sup>) Moreover, it is possible that the presence of the vortex induces separation, and a separated bubble that could drift on the surface of the airfoil following the path of the free vortex. Such a bubble could reduce the magnitude of the peaks in the pressure distribution and the lift history.

In a more recent paper, Booth<sup>31</sup> readjusts the scale on his data. According to this report, peaks B and C correspond to values of the lift coefficient of  $0.08$  and  $-0.13$ , respectively. These compare a little more favorably with our prediction  $C_2 = 0.11$  and  $-0.75$ , respectively. However, more accuracy is certainly desirable for such predictions.

Comparisons of the same type of lift variations with the calculations of Ref. 8 are displayed in Figs. 15 and 16. There is some qualitative agreement, but the sharp positive peak is missing from the results of Hsu and Wu<sup>8</sup> (Fig. 16). The two methods are very similar, and therefore the discrepancy cannot be explained. Neither is this discrepancy explained by examining the strength of the nascent vortices shed at the trailing edge. The history of the strength of nascent vortices is displayed in Figs. 17 and 18, and it appears clearly that the two methods predict a very similar behavior of this aspect of the flow.

### Conclusions

The present calculations indicate that the passage of a vortex generates fluctuations on the lift of the airfoil with a period much smaller than the time required for the vortex to traverse the distance from the leading to the trailing edge. This finding is in qualitative agreement with earlier experimental results. For design purposes, therefore, it is important to anticipate forcing frequencies higher than the frequency of vortex passage.

The method of discrete vortex dynamics proved quite adequate for describing this complex phenomenon, at least as far as the temporal sequence of events is concerned. A vortex approaching the blade at a level close to its leading edge will probably be cut. This effect is not modeled by the present theory. Nevertheless, it appears that if the vortex center passes just 0.05 chord above or below the airfoil, the results of the present theory predict with reasonable accuracy the temporal variations of lift.

### Acknowledgments

The initial stages of this work were completed under the sponsorship of NASA Grant NGT-47-004-801 while the first author was at VPI & SU. The authors acknowledge the interest and support of Drs. E. C. Yates and W. J. McCroskey, who have at times served as monitors of the project. Moreover, the advice of Dr. D. Mathioulakis with respect to the development of the computer code is acknowledged. The authors also wish to acknowledge the assistance of Mr. E. R. Booth of NASA Langley Research Center in providing pressure data for which test/theory correlations were made.

### References

- <sup>1</sup>McCroskey, W. J. and Goorjian, P. M., "Interactions of Airfoils with Gusts and Concentrated Vortices in Unsteady Transonic Flow," AIAA Paper 83-1691, July 1983.
- <sup>2</sup>George, A. R. and Chang, S. B., "Noise Due to Transonic Blade-Vortex Interactions," American Helicopter Society, Alexandria, VA, AHS Paper A83-39-50-D000, 1983.
- <sup>3</sup>Srinivasan, G. R., McCroskey, W. J. and Kutler, P., "Numerical Simulation of the Interaction of a Vortex with a Stationary Airfoil in Transonic Flow," AIAA Paper 84-0254, Jan. 1984.
- <sup>4</sup>Srinivasan, G. R., McCroskey, W. J., and Baeder, J. D., "Aerodynamics of Two-Dimensional Blade-Vortex Interaction," AIAA Paper 85-1560, July 1985.
- <sup>5</sup>Sankar, L. N. and Malone, J. B., "Unsteady Transonic Full Potential Solutions for Airfoils Encountering Vortices and Gust," AIAA Paper 85-1710, July 1985.
- <sup>6</sup>Wu, J. C., Sankar, L. N., and Hsu, T. M., "Unsteady Aerodynamics of an Airfoil Encountering a Passing Vortex," AIAA Paper 85-0202, Jan. 1985.
- <sup>7</sup>Wu, J. C., Hsu, T. M., Tang, W., and Sankar, L. N., "Viscous Flow Results for the Vortex-Airfoil Interaction Problem," AIAA Paper 85-4053, 1985.
- <sup>8</sup>Hsu, T. M. and Wu, J. C., "Theoretical and Numerical Studies of a Vortex-Airfoil Interaction Problem," AIAA Paper 86-1094, May 1986.
- <sup>9</sup>Mook, D. T. and Alexander, D. M., "On the Numerical Simulation of the Unsteady Wake Behind an Airfoil," AIAA Paper 87-0190, Jan. 1987.
- <sup>10</sup>Panaras, A. G., "Numerical Modeling of the Vortex/Airfoil Interaction," *AIAA Journal*, Vol. 25, Jan. 1987, pp. 5-11.
- <sup>11</sup>Booth, E. R., Jr. and Yu, J. C., "Two-Dimensional Blade-Vortex Interaction Flow Visualization Investigation," AIAA Paper 84-2307, Oct. 1984.
- <sup>12</sup>Booth, E. R., Jr., "Surface Pressure Measurement During Low Speed Two-Dimensional Blade-Vortex Interaction," AIAA Paper 86-1856, July 1986.
- <sup>13</sup>Favier, D., Castex, A., and Maresca, C., "Unsteady Characteristics of an Airfoil Interacting with a Vortical Wake," AIAA Paper 85-1707, July 1985.
- <sup>14</sup>Poling, D. R. and Telionis, D. P., "The Response of Airfoils to Periodic Disturbances—The Unsteady Kutta Condition," *AIAA Journal*, Vol. 24, Feb. 1986, pp. 931-199.
- <sup>15</sup>Ziada, S. and Rockwell, D., "Vortex-Leading-Edge Interaction," *Journal of Fluid Mechanics*, Vol. 118, May 1982, pp. 79-107.
- <sup>16</sup>Basu, B. C. and Hancock, G. J., "The Unsteady Motion of a Two-Dimensional Aerofoil in Incompressible Inviscid Flow," *Journal of Fluid Mechanics*, Vol. 87, July 1978, pp. 159-178.
- <sup>17</sup>Kim, M. J. and Mook, D. T., "Application of Continuous Vorticity Panels to General Unsteady Two-Dimensional Lifting Flows," AIAA Paper 85-0282, Jan. 1985.
- <sup>18</sup>Kemp, N. H. and Sears, W. R., "The Unsteady Forces Due to Viscous Wakes in Turbomachines," *Journal of Aeronautical Sciences*, Vol. 22, July 1955, pp. 478-483.
- <sup>19</sup>von Kármán, Th. and Sears, W. R., "Airfoil Theory for Nonuniform Motion," *Journal of Aeronautical Sciences*, Vol. 5, Aug. 1938, pp. 6-17.
- <sup>20</sup>Sears, W. R., "Some Aspects of Non-Stationary Airfoil Theory and Its Practical Application," *Journal of Aeronautical Sciences*, Vol. 8, Jan. 1941, pp. 43-47.
- <sup>21</sup>Milne-Thompson, L. M., *Theoretical Hydrodynamics*, McMillan, 4th ed., New York, 1960.
- <sup>22</sup>Giesing, J. P., "Vorticity and Kutta Condition for Unsteady Multi-Energy Flow," *Journal of Applied Mechanics*, Vol. 36, Sept. 1969, pp. 608-613.
- <sup>23</sup>Ham, N. D., "Aerodynamic Loading on a Two-Dimensional Airfoil During Dynamic Stall," *AIAA Journal*, Vol. 5, Oct. 1968, pp. 1927-1934.
- <sup>24</sup>Mathioulakis, D. S. and Telionis, D. P., "Modeling Rotating Stall by Vortex-Dynamics," AIAA Paper 83-0002, Jan. 1983.
- <sup>25</sup>Poling, D. R. and Telionis, D. P., "The Trailing Edge of a Pitching Airfoil at High Reduced Frequencies," *ASME Journal of Fluids Engineering*, Vol. 109, Dec. 1987, pp. 410-414.
- <sup>26</sup>Poling, D. R., "Airfoil Response to Periodic Disturbances—The Unsteady Kutta Condition," Ph.D. Dissertation, Virginia Polytechnic Institute and State Univ., Blacksburg, VA, Aug. 1985.
- <sup>27</sup>Sarpkaya, T. and Schoaff, R. L., "Inviscid Model of Two-Dimensional Vortex Shedding by a Circular Cylinder," *AIAA Journal*, Vol. 17, Nov. 1979, pp. 1193-1200.
- <sup>28</sup>Dadone, L., "The Role of Analysis in the Aerodynamic Design of Advanced Rotors," AGARD CPP 334, 1982, pp. 1-9.
- <sup>29</sup>Lee, D. J. and Smith, C. A., "Distortion of the Vortex Core During Blade/Vortex Interaction," AIAA Paper 87-1243, June 1987.
- <sup>30</sup>Poling, D. R., Wilder, M. C., and Telionis, D. P., "Two-Dimensional Interaction of Vortices with a Blade," AIAA Paper 88-0044, Jan. 1988.
- <sup>31</sup>Booth, E. R., Jr., "Experimental Observations of Two Dimensional Blade-Vortex Interaction," AIAA Paper 87-2745, 1987.